THE ION DRIFT METER FOR DYNAMICS EXPLORER-B

R. A. HEELIS, W. B. HANSON, C. R. LIPPINCOTT, D. R. ZUCCARO,
L. H. HARMON, B. J. HOLT, J. E. DOHERTY, and R. A. POWER

*Center for Space Sciences, Physics Program, The University of Texas at Dallas,
Richardson, TX 75080, U.S.A.*

(Received 11 May, 1981)

Abstract. The Ion Drift Meter on Dynamics Explorer-B measures two mutually perpendicular angles of arrival of thermal ions with respect to the sensor look direction. These measurements are used to derive two components of the ambient thermal ion drift velocity, which together with the third component from the Retarding Potential Analyzer instrument provide the total velocity. The Ion Drift Meter technique yields high temporal resolution measurements essential in the studies of the convection pattern and energy deposition in the ionosphere.

1. Introduction

An overview of the Dynamics Explorer program is given by Hoffman and Schmerling [1]. Fulfillment of many of the scientific objectives of this mission requires a knowledge of the motion of the ionospheric plasma. Motion of the ionospheric ions is important to their distribution, composition and temperature [2]. Rapid motion affects the ion temperature by Joule heating and the ion composition because chemical reaction rates are dependent on the relative velocity between ions and neutral particles. Convective motion can transport ions at high concentrations from the dayside to the nightside of the high latitude ionosphere and significantly affect the concentrations that might be expected from simple solar and particle production. Motion of the ions parallel to the earth's magnetic field may in some cases constitute a net current while in others it may provide a means of storing plasma during the day [3].

The component of the ion motion perpendicular to the earth's magnetic field is, of course, derivable from an electric and magnetic field measurement. However, parallel to the magnetic field, the electrostatic field and the ion drift velocity are not simply related and constitute quite different geophysical parameters. Measurement of the ion drift velocity vector is made by the Retarding Potential Analyzer (RPA) and the Ion Drift Meter (IDM) on DE-B. These instruments are mounted so that they look along the spacecraft X axis. Figure 1a shows the relationship between the direction of the incoming ions with respect to the spacecraft and the spacecraft axes X, Y, and Z. In the spacecraft frame the ion velocity V is made up of the ambient ion velocity V^i and the spacecraft velocity V^S. The velocity components parallel and perpendicular to the sensor look direction, $V_\parallel$ and $V_\perp$, are determined by the RPA and IDM respectively. The RPA is described in detail by Hanson *et al.* [4]. The ion velocity perpendicular to the sensor look direction is made up of two components along the Y and Z axes of the spacecraft. Figure 1(b) shows a projection onto the XZ plane of the situation in Figure 1(a) and illustrates the relationship

Space Science Instrumentation **5** (1981) 511–521. 0377–7936/81/0054–0511 $01.65.
Copyright © 1981 *by D. Reidel Publishing Company.*

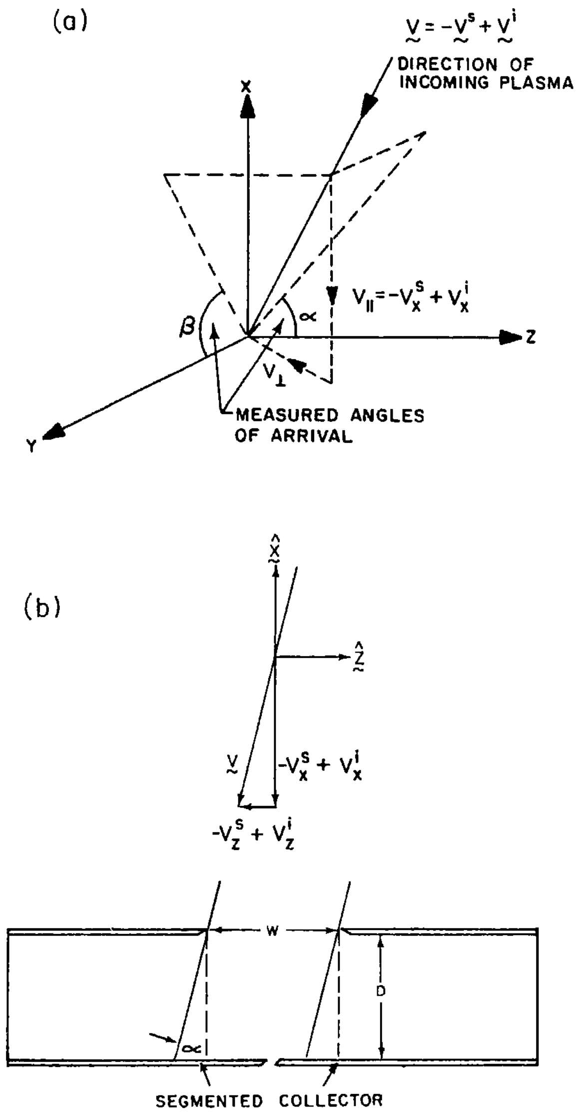

Fig. 1. A three-dimensional view and 1 dimensional projection of the geometry involved in ion arrival angle measurements by the IDM.

$$-V_Z{}^S + V_Z{}^i = (-V_X{}^S + V_X{}^i)\tan\alpha = V_{\|}\tan\alpha$$

that is used to determine $V_Z{}^i$. A similar relationship between $V_Y{}^i$, $\tan\beta$ and $V_{\|}$ is used to determine $V_Y{}^i$. The segmented collector shown in Figure 1(b) illustrates that a natural asymmetry in the current to opposite collector segments results if α is non-zero. Since the ion current to the collector is proportional to the irradiated area it can be shown that the ratio R of currents to each collector pair is given by

$$R = \frac{W/2 + D \tan \alpha}{W/2 - D \tan \alpha}.$$

The IDM determines the current ratio R to measure the arrival angle α. By utilizing 4 collector segments connected in pairs a similar geometry in the XY plane can be established and the angle β can be determined. It can be seen that the spacecraft velocity along the X, Y, and Z axes as well as the ambient ion drift velocity along the X axis is required to determine V_Y and V_Z from α and β. Thus, knowledge of the spacecraft attitude and the RPA derived component of ion velocity is required to produce V_Y and V_Z with their smallest error.

2. Instrumentation

The IDM for DE-B is very similar in design to those used successfully on the AE satellites [5]. A sensor consists of a square entrance aperture that serves as a collimator, some electrically isolating grids and a segmented planar collector. The angle of arrival of the ions with respect to the sensor is determined by measuring the ratio of the currents to the different collector segments. This ratio is determined by taking the difference in the logarithms of the current. We use two techniques to determine this ratio. In the first, called the standard drift sensor (SDS), the collector segments are connected in pairs to two logarithmic amplifiers. These log amplifiers provide the inputs to a single linear difference amplifier that measures either a horizontal arrival angle or the vertical arrival angle. The logarithmic amplifiers have a 5 decade dynamic range measuring currents from 10^{-11} to 10^{-6} A. The linear difference amplifier has three sensitivity ranges with sensitivities successively differing by a factor of 4, which provides a total dynamic range equivalent to about plus to minus 50 deg in ion arrival angle. This technique is described in detail by Hanson and Heelis [6]. It has the advantage that absolute differences between the log electrometers can be eliminated by a rezeroing technique, but a disadvantage that the horizontal and vertical arrival angles cannot be determined simultaneously. In addition, this technique involves some switching at the collectors themselves and thus the collectors are maintained at ground potential to minimize the effects of electrical transients.

The desire to perform the horizontal and vertical measurements simultaneously and to have the ability to bias the collector above and below ground potential in order to investigate other instrument characteristics led to the design of an alternative technique called the universal drift sensor (UDS). With this technique each collector segment is permanently connected to a logarithmic amplifier and two difference amplifiers are used to determine the horizontal and vertical arrival angles simultaneously. The logarithmic amplifiers are identical to those used in the SDS. The difference amplifiers have four ranges each different by $\sqrt{10}$ so that a total dynamic range equivalent to about plus to minus 50 deg in ion arrival angle is again available. The UDS advantage of simultaneity in angle measurements is compromised by the fact that absolute differences between the electrometers cannot be eliminated from the difference amplifier output. The IDM

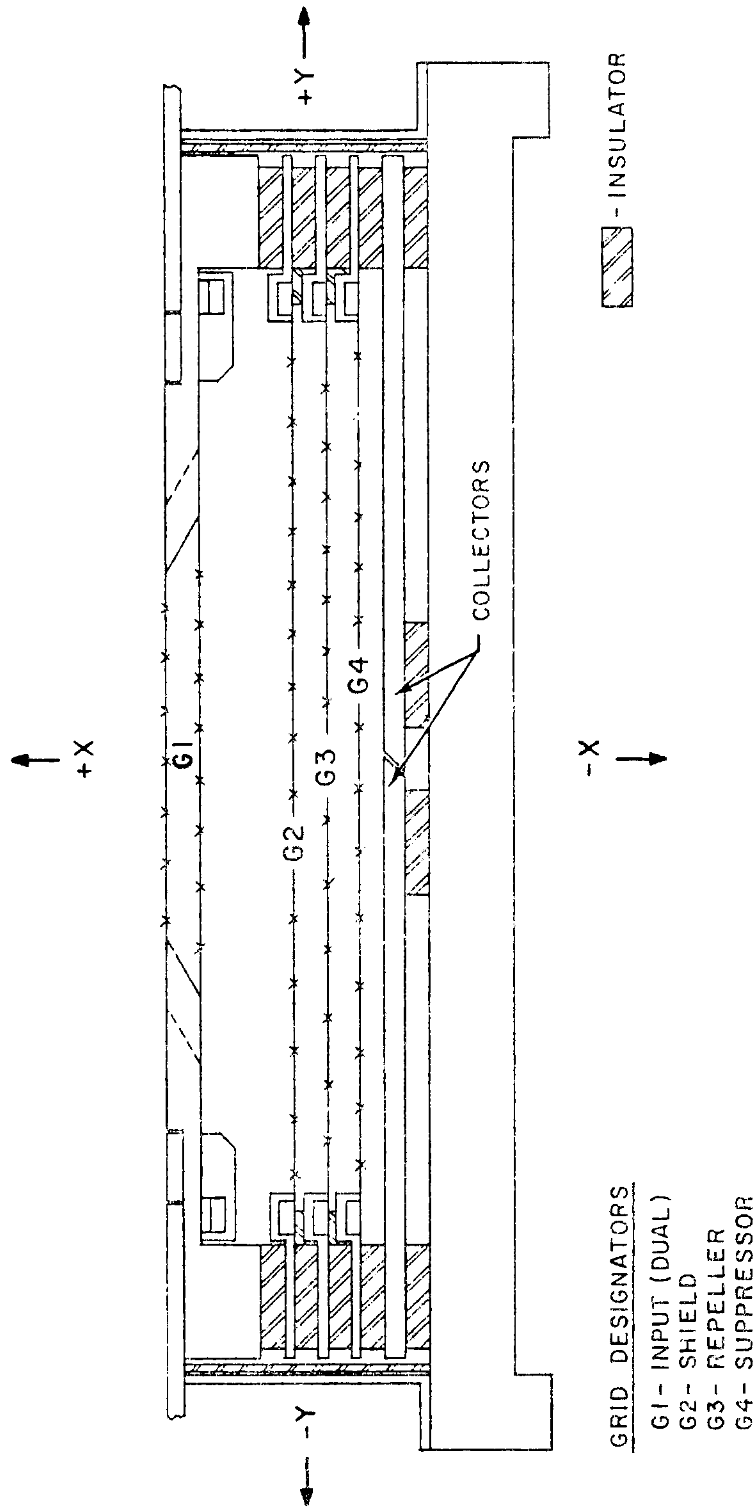

Fig. 2. Schematic cross-section of the IDM sensor showing the grid configuration and segmented collector.

consists of two sensors – one providing the SDS output and the other providing the UDS output. Each sensor is provided with 4 main frame telemetry words for analog signals and a digital word providing range and instrument function information. For each sensor the difference amplifier output is telemetered as the primary signal that is almost directly proportional to the ion arrival angle. Sampling of this output is preceded by a sequence of operations that are synchronized to the telemetry and are different for the SDS and the UDS.

Mechanically, the size and grid arrangements for the two sensors are identical and are shown in cross-section in Figure 2. The entrance apertures are covered by double grids, G_1, that are grounded and surrounded by a flat gold plated ground plane to ensure that transverse electric fields are minimized inside and outside the sensor. The grid G_2 is always grounded in the SDS to provide a field free drift space inside the instrument. In the UDS different potentials are applied to this grid to investigate the effects of spurious currents that will be described later. The instrument sensitivity can be drastically changed when hydrogen ions are present, since their random thermal velocity is comparable to the spacecraft velocity [6]. While correction for this sensitivity change can be made, O^+ ions are almost always present to allow a signal from ions whose random thermal velocity

TABLE I

Instrument summary

Weight Electronics box		2.20 kg
Sensors		1.70 kg
	Total	3.90 kg
Power		3.5 W
Telemetry		1.28 kbps

Grid biases	SDS	UDS		
		Ions	Neutrals	Electrons
Collector	0	−2	+17	−2
Suppressor G_4	−15	−15	−15	−15
Repeller G_3	0–3.75	0–3.75	0–3.75	0–3.75
Shield G_2	0	0	+15	+15
Input G_1	0	0	0	0

Geophysical parameters	Range	Accuracy	Nominal resolution
Transverse horizontal ion drift	-4 km s^{-1} to $+4$ km s^{-1}	± 50 m s^{-1} [a]	1/32 s
Transverse vertical ion drift	-4 km s^{-1} to $+4$ km s^{-1}	± 50 m s^{-1}	1/32 s

[a] The instrument sensitivity is about 3 m s^{-1} and an accuracy of 50 m s^{-1} is determined from the expected accuracy in vehicle attitude determination of about 0.5 deg.

is much smaller than the spacecraft velocity. Thus grid G_3 may be biased at a smaller positive potential to prevent hydrogen ions from striking the collector. Grid G_4 is always biased at -15 V to prevent thermal electrons from striking the collector and to suppress photo-emission from the collector. The collector itself is grounded in the SDS, whereas in the UDS it is biased at -2 or $+17$ V, depending on its mode of operation. A summary of the instruments' characteristics and functions is given in Table I.

2.1. SDS Operation

As was pointed out earlier, the SDS has the advantage that absolute differences between the logarithmic amplifiers can be removed from the arrival angle determination. These differences are removed by performing a 'rezero' and 'offset' sequence. During a 'rezero' operation the output of the difference amplifier is stored in a capacitor and this value is set to the middle of the telemetry band (2.5 V) to ensure maximum sensitivity to subsequent deviations of either sign. The inputs to the logarithmic amplifiers are then interchanged and the difference amplifier output relative to the capacitor value is telemetered. Thus a value equal to twice the absolute 'offset' between the two logarithmic amplifiers is telemetered. Following this offset operation the original logarithmic amplifier inputs are re-established and values relative to the rezero value are telemetered until the sequence is repeated. During the rezero and offset sequences the difference amplifier input passes through a 3 pole Bessel filter that is 3 dB down at 270 Hz to lessen the effects of switching transients. Subsequently a slower filter that is 3 dB down at 27 Hz is used to prevent aliasing at the sample rate. Ground commands are used to determine if the rezero and offset sequence occupies 1/8 or 1/16 s and to set the repeat frequency for rezero and offset sequences to 1/8 or 8 s. During these operations any one of 16 positive bias voltages between 0 to $+3.75$ V in 0.25 V increments can be selected by ground command and applied to grid G_3 to prevent H^+ ions from striking the collector. In general this grid will either be grounded or have the minimum voltage necessary to retard H^+ ions applied to it. In addition, ground commands are available so that the collector configuration for rezero and offset sequences and subsequent relative arrival angles may alternate between horizontal and vertical angles or be fixed on either one. If the rezero and offset sequence is repeated only every 8 seconds there is a substantial period during which there is no collector or electronic switching, and the absence of transients from these operations makes the data amenable to power spectral analysis. The RPA has associated with it a series of 6 filters covering the range 64 Hz to 8.5 KHz in factors of e, and it will be possible to share the lower 5 of these filters between the total ion current measured by the SDS. Thus a measure of the small-scale structure in the velocity will be available. Details of the filter bank are described more fully by Hanson *et al.* [4].

2.2. UDS Operation

For this sensor great care has been taken to remove any offsets between the logarithmic amplifiers that might be interpreted as ambient ion drifts. Nevertheless, precautions must be taken to ensure that such offsets do not adversely affect the signal and prevent us from making use of the instrument sensitivity. In order to ensure such sensitivity the difference amplifier output is periodically grounded through a capacitor and the telemetry output is set to the middle of the telemetry band. Subsequently the difference amplifier output is monitored relative to the newly established 'zero' on the capacitor and with maximum sensitivity to deviations of either sign. During this zero operation the absolute output of each logarithmic amplifier is also telemetered. The 'zero' operation occupies 1/16 s and is repeated every 8 s. Since only single collector segments supply the inputs to the difference amplifiers, there are always two collector pairs that provide horizontal or vertical arrival angles. The UDS provides automatic selection of a collector segment pair for a given arrival angle direction by determining the collector segment with the largest current and selecting it and the appropriate adjacent quadrant. The capability also exists to override the automatic collector selection in case of failure and to determine the characteristics of all the logarithmic amplifiers. It is, therefore, possible to select a given collector segment and the appropriate adjacent quadrant by ground command. Ground commands are also used to enable each difference amplifier to be configured for horizontal ion arrival angles only, vertical ion arrival angles only, or to alternate between horizontal and vertical at the 'zero' sequence repeat rate (8 s). As with the SDS any one of 16 positive bias voltages between 0 and + 3.75 V in 0.25 V increments can be selected by ground command and applied to the repeller grid G_3 to prevent H^+ ions from striking the collector.

It has been well established in data from the Atmosphere Explorer satellites that neutral particle impacts on the drift meter collectors can produce ion emission that can distort the output signal and in some cases completely dominate the ambient ion current [4]. These net negative currents can be measured with the UDS. Here the shield grid G_2 is biased at + 15 V to prevent ambient ions from striking the collector. The collector is biased at + 17 V to ensure that any ions leaving the collector can overcome the + 15 V shield grid potential and not return to the collector and the suppressor grid is maintained at − 15 V. In this configuration we are able to measure the absolute ion currents produced by neutral particle impact. In addition, if the ion emission from the collectors is uniform across the collector surface, the difference amplifier output should be proportional to the neutral particle arrival angle and hence to the transverse neutral drift velocity. While we have limited confidence that this mode will produce geophysical data, it might provide excellent data concerning the nature of these background currents.

Negative collector currents also result from energetic electrons and photoelectrons that strike the collectors. We are able to assess the effect of these signals on our data by using the previous grid voltage configuration except that the collector is biased at − 2 V to suppress the liberation of ions discussed above.

In all the above functions the 8 s cycle time described at the beginning of the UDS description is preserved. However, in recognition of the fact that there is a possibility of providing neutral particle drift data, a mode is also included that allows the UDS to alternate between ambient ion measurements and neutral particle measurements every 1/4 s.

In principle the UDS is capable of providing simultaneous horizontal and vertical ion

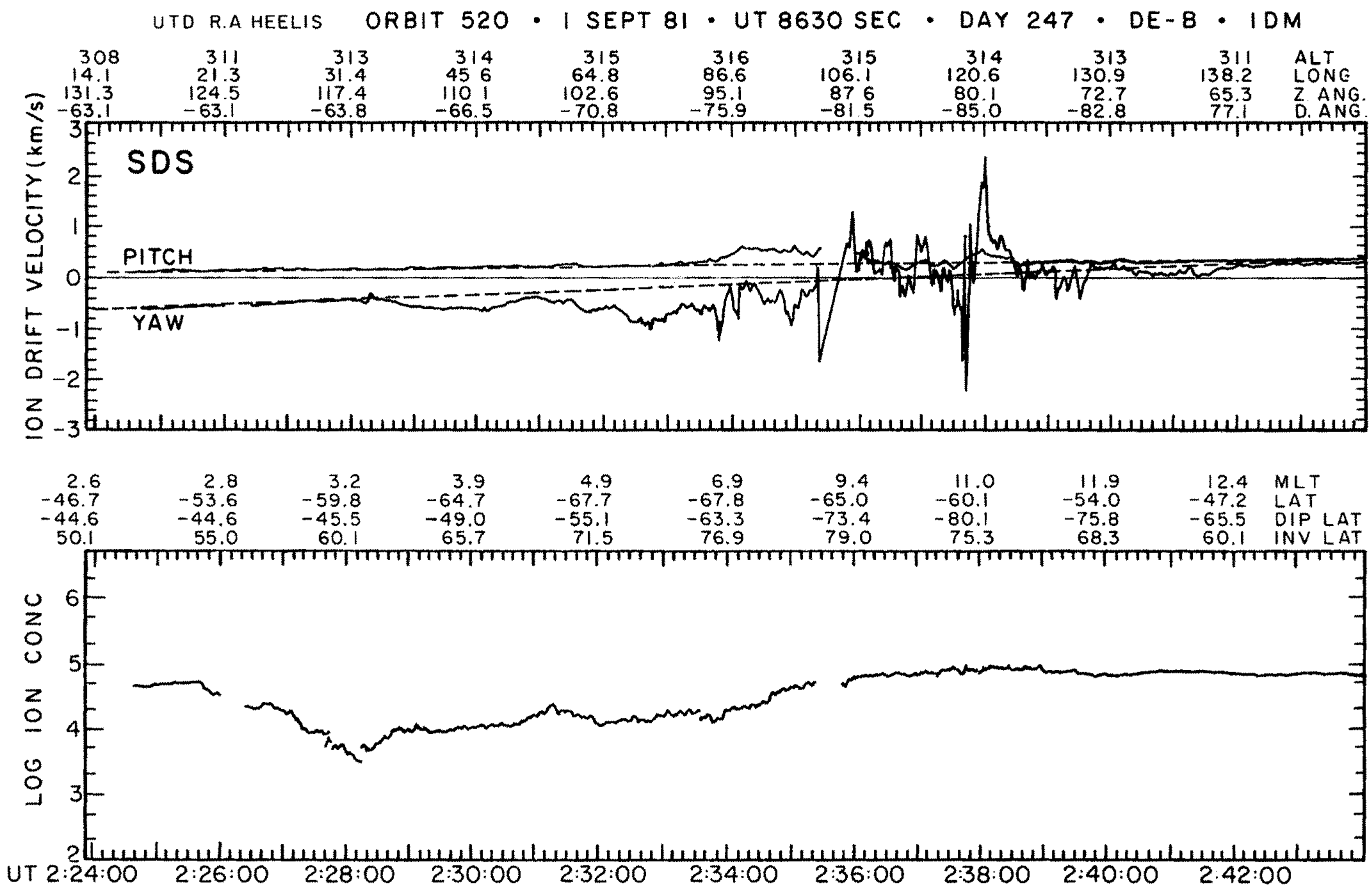

Fig. 3. Typical example of expected ion drift velocity output as a function of time along the satellite track. Data from Atmosphere Explorer are used to illustrate the variations that can be expected. Pitch and yaw traces will be identified by different line patterns.

arrival angle data, although the technique has not been tried before. In the unlikely event that this proves to be superior to the SDS sensor or that the SDS sensor should fail, we have the capability to assign all the telemetry to the UDS by ground command. In this mode we can regain the 1/64 s resolution on simultaneous measurements available from operating the UDS and SDS in tandem.

3. Data Presentation

Routine data processing from both UDS and SDS will be performed by programs run on the Science Data Processing System. Microfilm/microfiche displays will be the primary source of visual data; Figure 3 shows a typical microfilm display. The data will initially be converted from arrival angle to drift velocity assuming the ram component of drift from the RPA is zero. In general the X component of the spacecraft velocity will be much larger than the same component of the ambient ion drift velocity and the error in the derived velocity components along the Y and Z axes will be quite small. The data are plotted independently for the UDS and the SDS and a 20 min frame will contain data points every 1/4 s. The data will be stored at this time base in the Mission Analysis Files (MAF's) [7]. In addition, when data are available at higher time resolution additional plot frames will be produced in 1 min frames. These high resolution data will not be stored in MAF's. The display will show one or two velocity components for SDS depending upon the instrument mode and differentiated by different line patterns. In addition the components of the spacecraft velocity relative to a corotating atmosphere along the two transverse axes Y and Z are also plotted. These will be labelled 'pitch' and 'yaw' respectively and are denoted by dashed lines in the figure.

The UDS display will show a maximum of four velocities corresponding to pitch and yaw angles measured by each difference amplifier. We expect that corresponding pitch and yaw values will be very close, but the ability to view them simultaneously will provide the integrity checks that are needed. In addition, the pitch and yaw data described previously will be plotted. Routine operations on the Mission Analysis Computing System (MACS) [7] will involve the generation of ion drift velocity vectors and their graphical presentation as line plots and on polar dials. Figure 4 shows an example of such a display. The three components of ion drift together with additional information available from the RPA and filter banks will be stored in a revised MAF. The displays from these routine operations will be produced on microfilm and microfiche. The displays shown in Figure 4 will also be available from a fully interactive graphics program available to DE investigators.

Acknowledgments

We would like to thank R. F. Bickel for his initial design of the instrument electronics and L. A. Swaim and J. C. Brown for technical support throughout the project.

The hardware effort ongoing and future software efforts are supported by NASA under contracts NAS5-24298, NAS5-26071, NAS5-24297 and NAS5-26068.

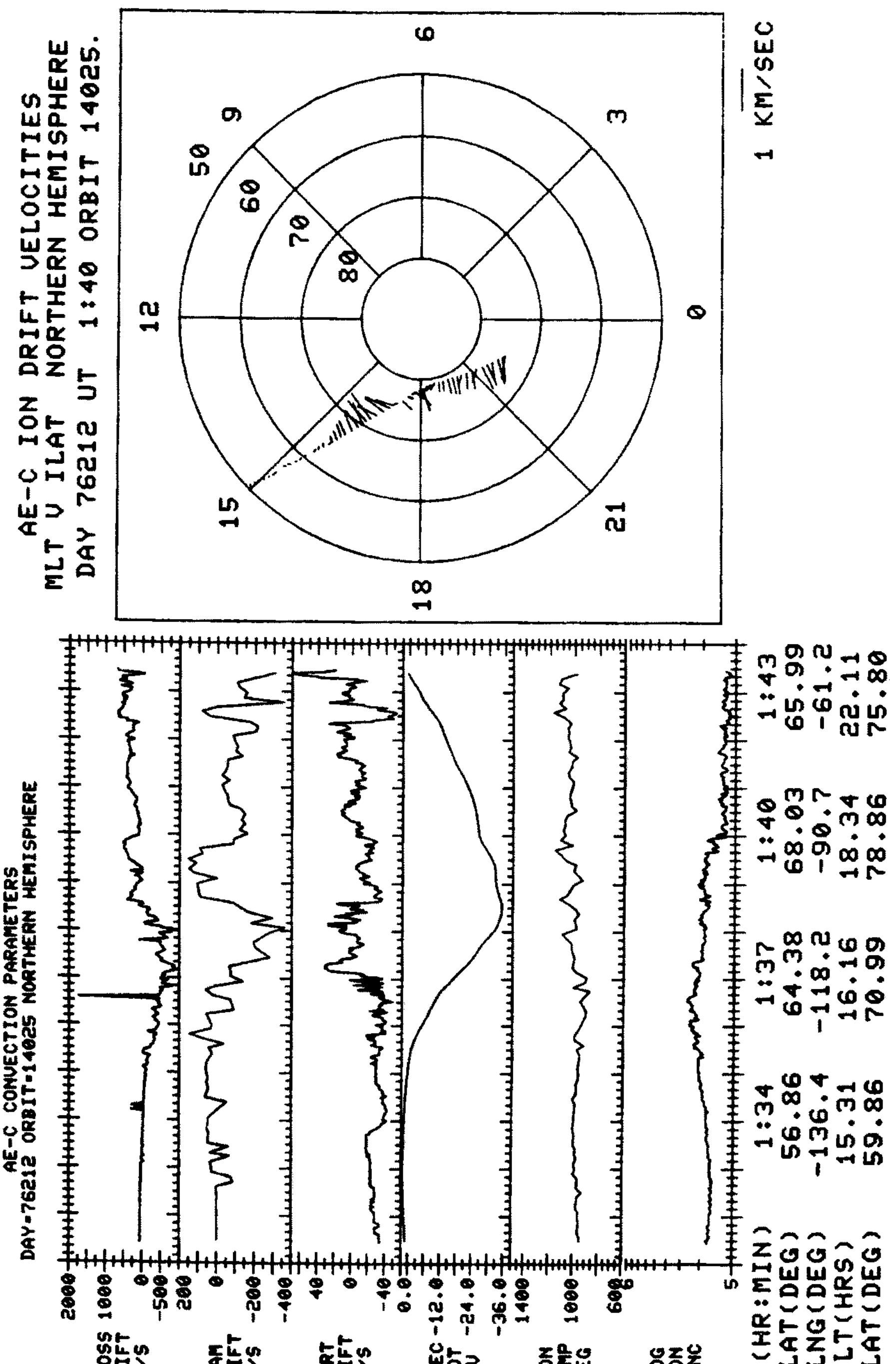

Fig. 4. Example of refined data display available from geophysical parameters derived from the IDM and RPA. Again Atmosphere Explorer data are used, but better resolution will be available from DE.

References

1. Hoffman, R. A. and Schmerling, E. R.: *Space Sci. Instrum.* **5**, 345 (1981) (this issue).
2. Schunk, R. W., Banks, P. M., and Raitt, W. J.: *J. Geophys. Res.* **81**, 3271 (1976).
3. Murphy, J. A., Bailey, G. J., and Moffet, R. J.: *J. Atmos. Terr. Phys.* **38**, 351 (1976).
4. Hanson, W. B., Heelis, R. A., Sanatani, S., Lippincott, C. R., Zuccaro, D. R., Harmon, L. L., Holt, B. J., Doherty, J. E., and Power, R. A.: *Space Sci. Instrum.* **5**, 503 (1981) (this ussue).
5. Hanson, W. B., Zuccaro, D. R., Lippincott, C. R., and Sanatani, S.: *Radio Sci.* **8**, 333 (1973).
6. Hanson, W. B. and Heelis, R. A.: *Space Sci. Instrum.* **1**, 493 (1975).
7. Smith, Paul H., Freeman, Clyde H., and Hoffman, R. A.: *Space Sci. Instrum.* **5**, 561 (1981) (this issue).